4ICEGE Thessaloniki-GREECE 2007

4th International Conference on
Earthquake Geotechnical Engineering
June 25-28, 2007
Paper No. 1699

DISPLACEMENT-METHODS FOR THE DESIGN OF EARTH RETAINING STRUCTURES

Sara VECCHIETTI [1], Manuela CECCONI [2], Vincenzo PANE [3]

ABSTRACT

Seismic design is currently based on force, rather than displacement. However, in the recent years, displacement-based approaches for seismic design have been proposed in the literature (Priestley and Kowalsky, 2000; Priestley, 2001). The paper focuses on the application of the Displacement-Based-Design (DBD approach) to retaining walls. The kernel of a such a procedure consists in choosing an appropriate equivalent SDOF "substitute structure", characterized by the effective secant stiffness K_e at maximum displacement (Δd), effective mass, m_e, and equivalent viscous damping, ξ_{eq}, (Gulkan and Sozen, 1974; Shibata and Sozen, 1976). The design (or maximum) displacement is set by the designer to ensure acceptable level of deformation for a given risk event.
The procedure has been originally applied to rigid retaining walls and flexible cantilever diaphragm walls in purely frictional granular soils. In the former case it has been assumed the mobilization of an active wedge behind the wall and a constant displacement pattern has been adopted and scaled until a limit displacement is reached. In the latter case, the first elastic vibration mode involving the whole height of the structure has been set as a first approximated deformed shape.
The results have been critically discussed and compared with those obtained from traditional pseudo-static analyses (Mononobe and Matsuo, 1929, Okabe, 1926).

Keywords: displacement based design method, retaining structures, Eurocodes 8

1. INTRODUCTION

The design procedure known as direct Displacement Based Design (DBD) method has been developed over the past ten years (Priestley, 1993, 2003) in the attempt to mitigate deficiencies in current force-base design techniques.

Historically, much research effort has been directed to evaluate the available ductility capacity of different structural systems, performing extensive experimental and analytical studies to determine their safe displacement capacity. However, the design process has been still carried out in terms of required strength in essentially all codes of practice around the world and displacement capacity, if directly checked at all, has come out at the end. In the last decade, however, several researchers proposed displacement-based approaches for earthquake engineering evaluation and design, with the aim of providing improved reliability in the engineering process by more directly comparing computed response and expected structural performance.

[1] Ph.D. Student, Department of Civil and Environmental Engineering, University of Perugia, Italy, Email: sara.vecchietti@unipg.it
[2] Assistant Professor, Department of Civil and Environmental Engineering, University of Perugia, Italy, Email: ceccon@unipg.it
[3] Full Professor, Department of Civil and Environmental Engineering, University of Perugia, Italy, Email: panev@unipg.it

Direct DBD represents the structure to be designed by a single-degree-of-freedom (SDOF) elastic equivalent system (Fig. 1a)). Since the actual structural behaviour is non-linear, the design process is made by assuming that the dynamic performance of the SDOF system is characterized by its maximum displacement response, rather than its initial tangent elastic properties. This concept is based on the substitute structure approach established by Gulkan and Sozen (1974) and Shibata and Sozen (1976).

The direct DBD procedure is illustrated in Figure 1, showing the design steps required for a frame-wall building (Sullivan *et al.*, 2005). However, the basic fundamentals apply to all structural types. At this point, a main question arises: *is direct DBD also suitable for geotechnical applications, such as retaining structures, foundations and slope stability problems?* The results presented in this paper are aimed to finding some hints to this issue, with regard to soil retaining structures. For this purpose, the general procedure needs to be described.

The bi-linear envelope of the lateral force-displacement response of a SDOF system is represented in Figure 1b), showing the secant equivalent stiffness K_e at the maximum displacement Δ_d. This value is set by the designer to ensure an acceptable level of displacement for a given risk event. Obviously, the choice of an acceptable deformation value leads to considering the damage of both structural and non-structural items.

An assumed displaced shape can be scaled until the most critical element in the structure reaches its limit displacement; the appropriate displaced shape could be that which corresponds to the inelastic first-mode at the design level of seismic excitation. Representing the displacement by the inelastic rather than the elastic first-mode shape is consistent with characterizing the structure by its secant stiffness to maximum response. Often, the inelastic and elastic first-mode shapes are very similar.

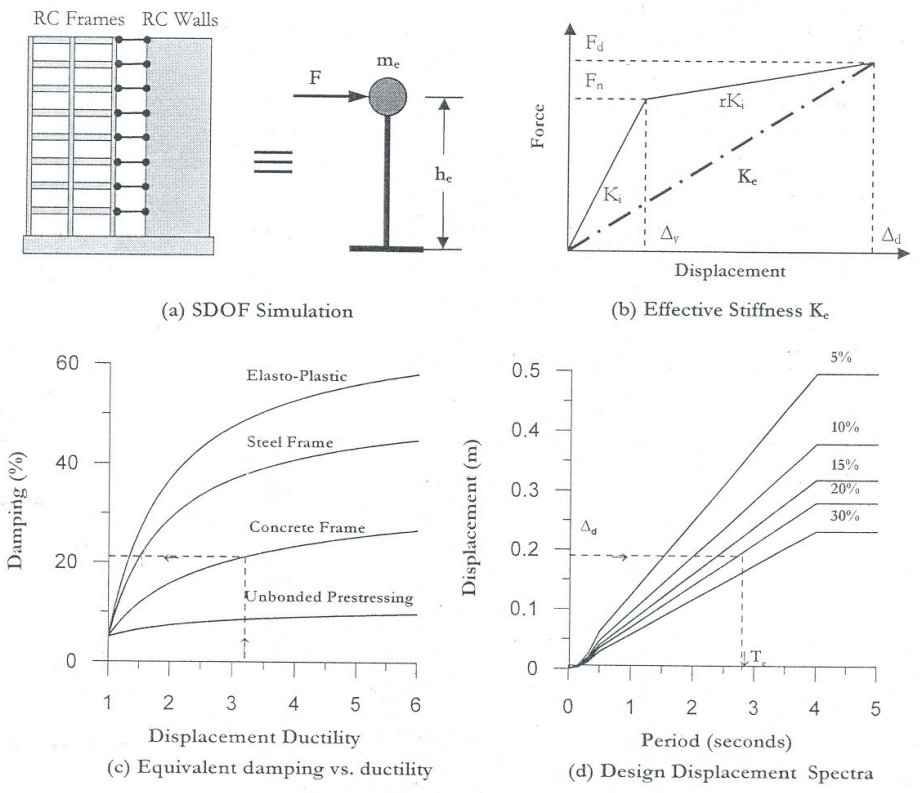

Figure 1. Fundamentals of the Direct DBD method (from Sullivan *et al.*, 2005)

When the displaced shape of the structure at maximum response is known, then the design displacement, Δ_d, can be obtained using the following equation:

$$\Delta_d = \frac{\sum_{i=1}^{n}(m_i \Delta_i^2)}{\sum_{i=1}^{n}(m_i \Delta_i)}. \quad (1)$$

For a multi-storey building, n represents the total number of storeys, with mass m_i and displacement Δ_i at the i^{th}-storey. For bridges, the mass locations will normally be at the top of the piers. The applicability of such a discretized mass approach for retaining structures is still uncertain and will be discussed in the following sections.

With regard to Figure 1a), the equivalent displacement corresponds to the design displacement at effective height, h_e, of the structure. As such, the effective height is also a function of the displaced shape of the masses at maximum response:

$$h_e = \frac{\sum_{i=1}^{n}(m_i \Delta_i h_i)}{\sum_{i=1}^{n}(m_i \Delta_i)}. \quad (2)$$

Since the real structural behaviour is non-linear, the effective stiffness is used combined with an equivalent viscous damping, ξ, representative of the hysteretic energy adsorbed during the seismic response. Figure 1c) shows the damping coefficient ξ as a function of the ductility demand for different structural systems.

The DBD design procedure can be performed according to the following steps (from Sullivan *et al*., 2005):

1. an elastic deformed shape of the structure at maximum response is established; analytical or empirical expression can be used to this attempt;
2. the design displacement and the effective height are calculated through Eqs. (1) and (2);
3. the effective mass, representing the mass participating in the first inelastic mode of vibration at maximum response, can be obtained from:

$$m_e = \frac{\sum_{i=1}^{n}(m_i \Delta_i)}{\Delta_d}; \quad (3)$$

4. from the expected level of ductility demand, the corresponding damping is evaluated for example from Fig. 1c). This matter is rather complex and challenging. It needs to be investigated for geotechnical applications;
5. the effective period T_e at maximum displacement response can be read – to the opinion of many researchers working in the field - from the elastic displacement spectra for different levels of damping, as shown in Fig. 1d).
6. the effective stiffness of the equivalent SDOF oscillator is then related to its period and mass according to:

$$T = 2\pi\sqrt{\frac{M}{K}} \rightarrow K_e = \frac{4\pi^2 m_e}{T_e^2} \quad (4)$$

7. finally, the design lateral force, F_d, equivalent to the design dynamic base force, V_b is given from:

$$V_b = K_e \Delta_d \; ; \tag{5}$$

8. the base shear can be finally distributed as equivalent lateral forces applied to the various discretized masses of the structure according to:

$$F_i = V_b \frac{m_i \Delta_i}{\sum_{i=1}^{n} m_i \Delta_i} \tag{6}$$

where F_i is the design force at i^{th} mass. These lateral forces may be used to establish the necessary strength of individual elements within the structure.

The calculation procedure appears to be simple. Nevertheless, many complexities arise when the method is applied to retaining structures. The definition of the "substitute structure", *i.e.* the mass discretization, or the evaluation of the function damping/ductility demand are the main questions to solve. On the other hand, the realistic assumption of an elastic deformed shape (step 1) for such geotechnical applications seems to be a minor problem.

With regard to the development of the elastic displacement spectra at different levels of viscous damping, the adopted approach is that of using the factor η, defined in the EUROCODE 8 (EN 1998-1) and given by:

$$\eta = \sqrt{10/(5+\xi)} \geq 0.55 \, . \tag{7}$$

Figure 2 shows the elastic response spectrum in terms of maximum acceleration (Fig. 2a) and maximum displacement (Fig. 2b). They are both expressed as functions of the vibration period of SDOF systems, according to the analytical equations reported in EC8. The numerical values of representative periods, that identify different portions of the response spectra are given in the Italian OPCM 2003 n.3274.

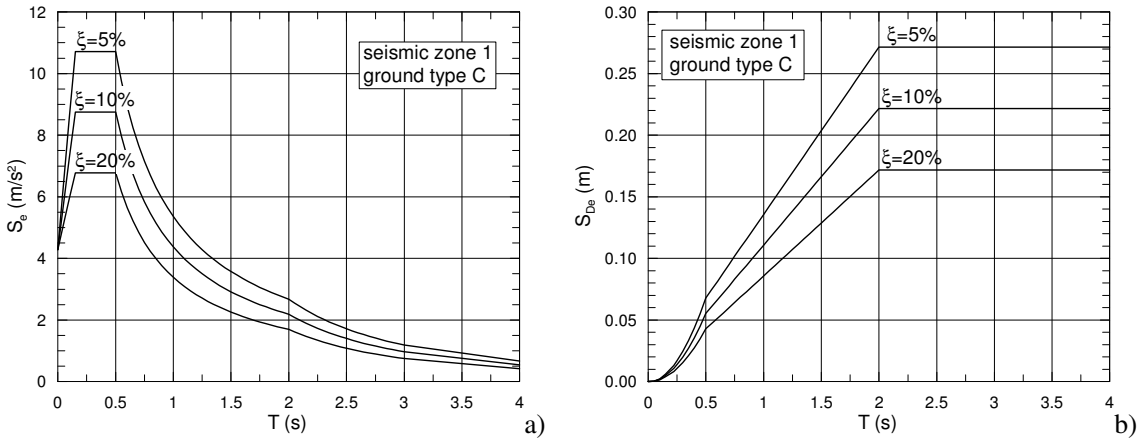

Figure 2. Elastic response spectra (from OCPM 2003, n. 3274)

The direct DBD design method has been applied to two main types of retaining structures, *i.e.* cantilever retaining walls and diaphragm walls. In the following section, the applicability of the design procedure is discussed in detail.

2. APPLICATION TO RETAINING WALLS

The geometry of the retaining structure is given very schematically in Figure 3. A concrete cantilever wall retains a cohesionless sandy backfill. The wall dimensions and the soil properties are given in Table 1. The following assumptions are made:

- the ground water is well below the base of the wall;
- the granular fill above the heel of the wall (placed after of the construction), the in-place backfill, and the foundation soil are characterised by the same physical-mechanical properties.

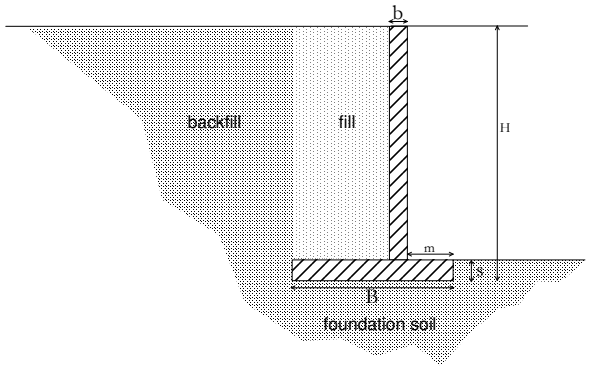

Figure 3. Geometry of the retaining wall

Table 1. Soil properties and walls geometry

SOIL	a_g/g	S	ϕ (°)	c (kPa)	δ [(1)] (°)	γ (kN/m^3)
medium dense sand (ground type C, V_s = 200m/s)	0.35	1.25	30	0	0, 2/3 ϕ, ϕ	20
WALLS	H (m)	B (m)	b (m)	m (m)	s (m)	γ_c (kN/m^3)
concrete cantilever retaining wall	6.0	4.7	0.7	1.2	0.8	25
diaphragm wall	4.0	/	0.6	/	/	25

(1) the value $\delta = 2/3\phi$ was assumed only for the diaphragm wall, see §3.

The calculations were made for the seismic zone 1 and the ground type *C*. In this case, according to the Eurocodes and the Italian OCPM 3274, the peak ground acceleration $a_g = 0.35g$ and the horizontal seismic coefficient,

$$k_h = \gamma_1 \frac{a_g \cdot S}{r} \tag{8}$$

where γ_1 is the importance factor ($\gamma_1 = 1$), S is the Soil factor ($S = 1.25$) and r represents a factor increasing from 1 up to 2 as the acceptable displacement increases. The r values are given in the EC8, EN 1998-5 (Table 7.1). However, as suggested by Simonelli (2005), there are still some doubts on the values of r to be adopted for walls than can accept large displacements. The values of r adopted in the analyses are those listed in Table 2, following the Authors interpretation of the mentioned Table 7.1 reported in EC8.

Table 2. Factor *r* affecting the horizontal seismic coefficient k_h (from Table 7.1 EN1998-5; revisited, to the Authors opinion)

TYPE OF RETAINING STRUCTURE ($\alpha = a_g\gamma/g$)	r
free gravity walls that can accept a displacement d_r > 300 αS (mm)	2.0
as above with 200 αS < d_r < 300 αS	1.5
flexural reinforced concrete walls…restrained basement walls	1.0

2.1 Design procedure

2.1.1 Participating masses

Figure 4 shows the assumed discretized equivalent system. The total mass of the structure includes the mass of the wall itself and the granular fill. The soil mass participating in the seismic action is conventionally represented by the active wedge with inclination α with respect to the horizontal plane. The i^{th} soil mass at a depth (H - z_i) from the ground table is then expressed by:

$$m_i(z_i) = \frac{\gamma z_i d_i}{\tan\alpha} \tag{9}$$

where z_i is the height of the centre of mass of the i^{th} soil layer of thickness d_i.

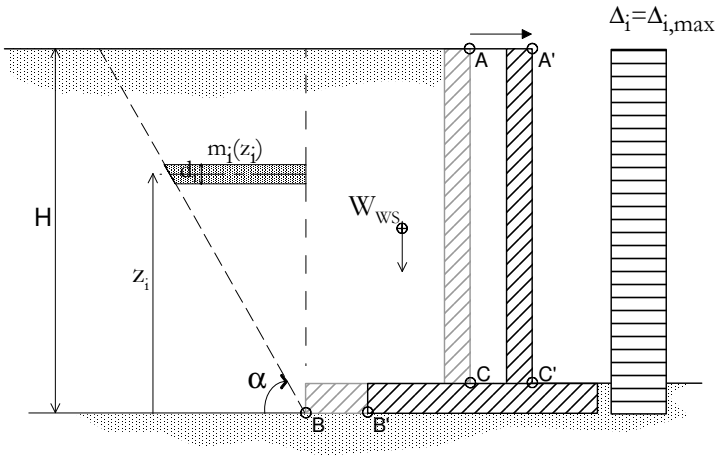

Figure 4. Discretized system of a soil retaining structure

A main subject of interest in the calculation procedure is the choice of angle α. This sensibly affects the values of dynamic base forces V_b. The flatter is the soil wedge, the larger is the dynamic force. Based on the pseudo-static analysis of seismic earth pressures on retaining walls performed by Okabe (1926) and Mononobe and Matsuo (1929) - popularly known as the Mononobe-Okabe method – and the derivation of the dynamic active earth pressure coefficient, K_{ae}, the critical failure surface delimiting the active wedge – for a horizontal ground table - is inclined at angle α (Zarrabi Kashani, 1979):

$$\alpha_{MO} = \phi - \psi + \tan^{-1}\left(\frac{-\tan(\phi-\psi)+C_1}{C_2}\right)$$

with
$$C_1 = \sqrt{\tan(\phi-\psi)\left[\tan(\phi-\psi)+\cot an(\phi-\psi)\right]\left[1+\tan(\delta+\psi)\cot an(\phi-\psi)\right]} \tag{10}$$
$$C_2 = 1+\left\{\tan(\delta+\psi))\left[\tan(\phi-\psi)+\cot(\phi-\psi)\right]\right\}$$

where ϕ is the soil friction angle, δ is the interface friction angle between the soil and the wall and $\psi = \arctan(k_h)$. For simplicity, it is assumed the vertical seismic coefficient $k_v = 0$. For the chosen soil properties and seismic zone parameters reported in Table 1, the value of angle α_{MO} is 29° (if δ=0). For comparison, it has also been assumed a value of α corresponding to the Coulomb critical plane surface in the active state ($\alpha_{COULOMB} = 45° + \phi/2 = 60°$, if δ=0).

2.1.2 Displacement pattern

The assumed elastic deformed shape of the structure (wall + soil) consists of a constant pattern of horizontal displacements (see Fig. 4), which is plausible for the rigid wall at hand. Implicitly, it is

assumed - for sake of simplicity - a pure translational mechanism of a single block formed by the structure and the soil wedge. Calculations were made through points 1-7 listed in §1. Then, the dynamic force V_b was distributed into equivalent lateral forces applied to the soil mass (V_s) and the wall (V_w), as follows:

$$V_s = V_b \frac{m_s \Delta_i}{\sum_{i=1}^{n} m_i \Delta_i}; \qquad V_w = V_b \frac{m_w \Delta_i}{\sum_{i=1}^{n} m_i \Delta_i}. \tag{11}$$

Figure 5 and 6 show the numerical results obtained from the analyses, in terms of dynamic base force V_b and maximum displacement $\Delta_{i,max}$. For a chosen constant value of the damping ratio, ξ = 10%, the results are synthesized in two plots, separately showing the effects of:

- the soil wedge angle α (Fig. 5);
- the friction angle at the interface backfill/wall, δ (Fig. 6)

on the dynamic forces V_b and V_s.

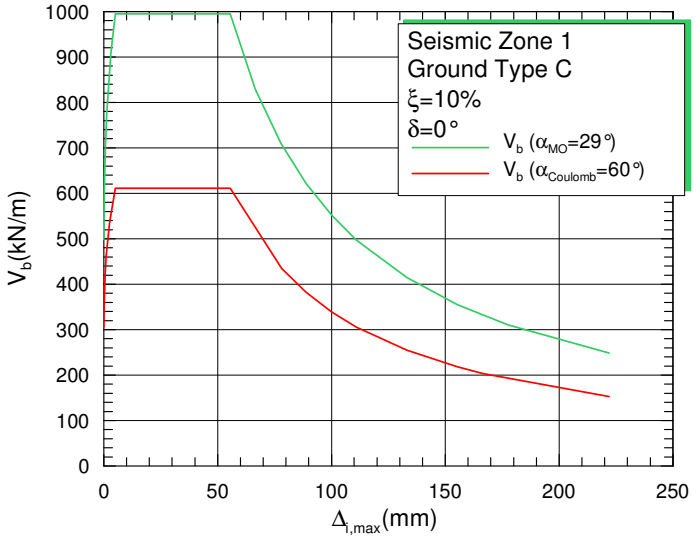

Figure 5. Dynamic force V_b *vs*. maximum displacement, $\Delta_{i,max}$ for different values of angle α

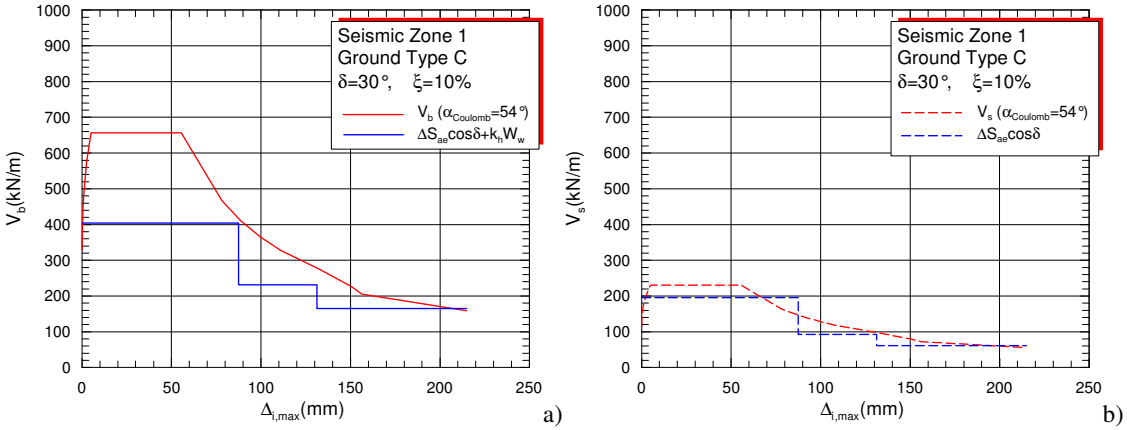

Figure 6. Dynamic forces V_b and V_s *vs*. max. displacement, $\Delta_{i,max}$ for δ= 30°

The trend of V_b reflects the shape of the acceleration response spectrum. For very small displacements, the dynamic force increases steeply to reach a constant value which persists for values of $\Delta_{i,max}$ in the range 10 – 50 mm. Then, a gentle decrease of V_b is accompanied to a gradual increase of the maximum displacement. In much detail, from Figure 5 it is noted that V_b strongly depends on the value of angle α. An increase of V_b of about the 67% is observed when α varies from 60° ($\alpha_{COULOMB}$) to 29°(α_{MO}). Thus, an adequate choice of the soil wedge geometry appears to be essential for the economy of design; this aspect of the procedure still needs some more investigation.

Figure 6a) shows the values of V_b for an interface friction angle, $\delta = 30°$. The horizontal line represents the dynamic active force increment ($\Delta S_{ae} + k_h W_w$) evaluated by using the MO pseudostatic analysis, which does not depend on the maximum displacement, while the stepped dashed-line represents the dynamic active force increment $\Delta S_{ae} + k_h W_w$ calculated by taking into account the factor r which increases with the amount of induced displacement, according to Table 2. In the hypothesis of $\alpha = \alpha_{COULOMB} = 54°$, it is noted that the results obtained from the DBD method are more conservative than those obtained with the pseudo-static analyses. This finding is not very surprising since, for the calculation of V_b, the elastic response spectrum is used in the derivation of Eqs. 4 and 5 (see step 5, §1). Moreover, from the comparison with Figure 5, a small increase of V_b is observed (of about 10%), when δ increases from 0 to 30°.

On the other hand, Figure 6b) shows the lateral force V_s, which is applied to the soil wedge, compared with the horizontal component of the dynamic active force increment $\Delta S_{ae}\cos\delta$. In this case, the results appear to be in fair agreement, and only in the range of small displacements, the DBD procedure is more conservative.

3. APPLICATION TO DIAPHRAGM WALLS

The discretized system assumed for the application of the DBD method to a diaphragm wall is shown in Figure 7. Very simply, the wall is supposed to be fixed at the base, with no rotation or horizontal/vertical displacements being permitted. Therefore, the wall behaves as a cantilever wall.

Also in this case, the soil mass participating in the seismic event is represented by the active soil wedge behind the wall. The weight of the structure is negligible with respect to the soil mass. The geometrical properties of the structure are reported in Table 1; the soil properties are the same previously assumed.

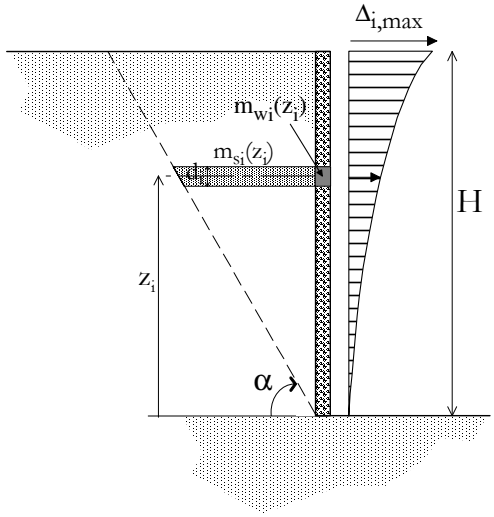

Figure 7. Discretized system of a diaphragm wall (simulated as a cantilever beam)

3.1 Design procedure

3.1.1 Displacement pattern

The deformed shape assumed for the diaphragm wall coincides with the 1st mode of vibration of a flexural-type cantilever beam. The maximum displacement $\Delta_{i,max}$ occurs at the top of the wall, and it attains a null value at the base. The analytical expression of the displacement function is reported in Appendix A.

3.1.2 Results

In Figures 8-10 the results of the DBD analyses are plotted once again in terms of dynamic forces V_b, V_s as a function of the maximum displacement $\Delta_{i,max}$, which occurs at the top of the wall. In the analyses, the inclination of the active soil wedge behind the wall is supposed to be simply $\alpha_{Coulomb}$. For the interface friction angle, it is assumed $\delta = 2/3\ \phi$, as recommended by EC8. In particular, Figure 8 shows clearly the relevant effect of the damping ratio, ξ on the values of the dynamic shear force. The values of V_b reduce with increasing ξ, while the amplitude of the range of $\Delta_{i,max}$ where V_b keeps a maximum constant value increases when ξ decreases.

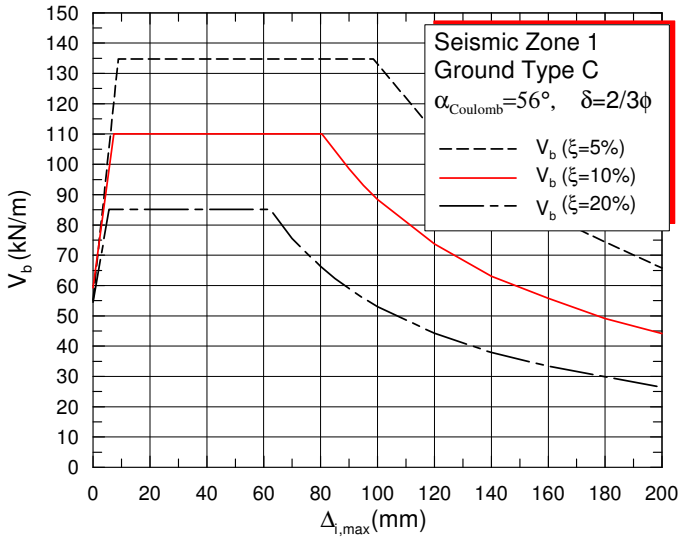

Figure 8. Dynamic force V_b *vs*. max. displacement $\Delta_{i,max}$ for different values of the damping ratio

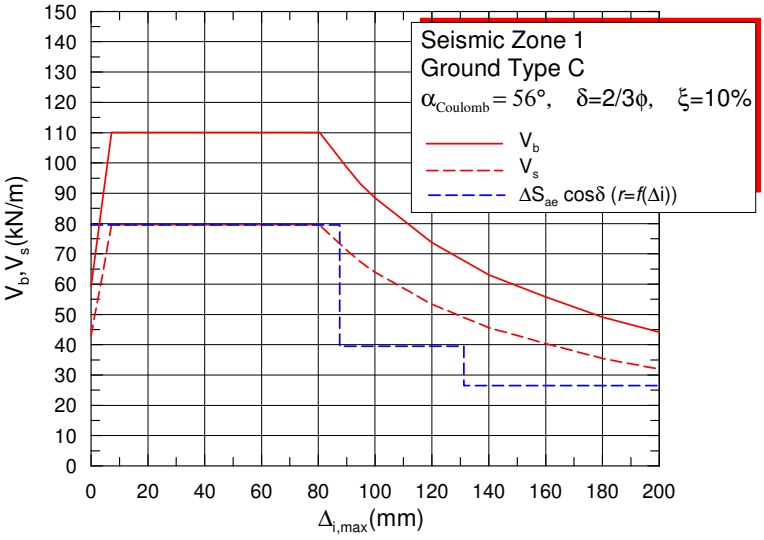

Figure 9. DBD method and MO pseudo-static analysis. Dynamic force V_s *vs*. $\Delta_{i,max}$

Figure 9 plots the results derived from DBD calculations compared with those obtained from pseudo-static analyses. In the range $10 < \Delta_{i,max} < 80$ mm, the values of the dynamic force V_s, applied to the soil wedge, are in good agreement with the values of the dynamic active force increment, $\Delta S_{ae}\cos\delta$, which in turn depends on the amount of induced displacement through the factor *r*. For larger displacements, the DBD procedure appears to be more conservative.

Finally, in order to improve the prediction of the dynamic force V_b in the small-displacement range of values, a variable soil damping ξ was assumed. In a first attempt, the average shear strain γ was approximately calculated as $\Delta_{i,max}/H$ (where H represents the total height of the wall), while the damping ratio-shear strain curve employed in the analyses is that reported in Figure 10a) and corresponding to $I_p = 0$ (cohesionless soils, see Table 1). From Figure 10b) it can be observed that the assumption of a variable soil damping ratio ξ allows to cut down the plateaux where the dynamic shear base forces V_b and V_s attain a constant value, leading to more plausible values, mainly in the range of small displacements (< 10 mm).

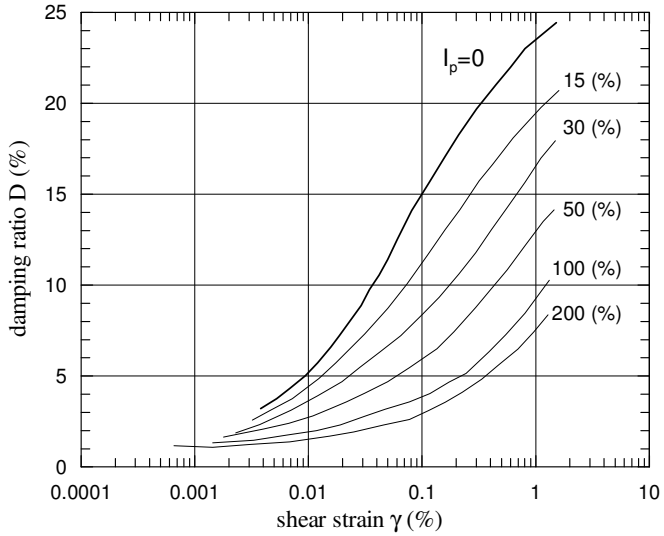

Figure 10a). Soil damping ratio against shear strain, γ (adapted from Vucetic and Dobry, 1991)

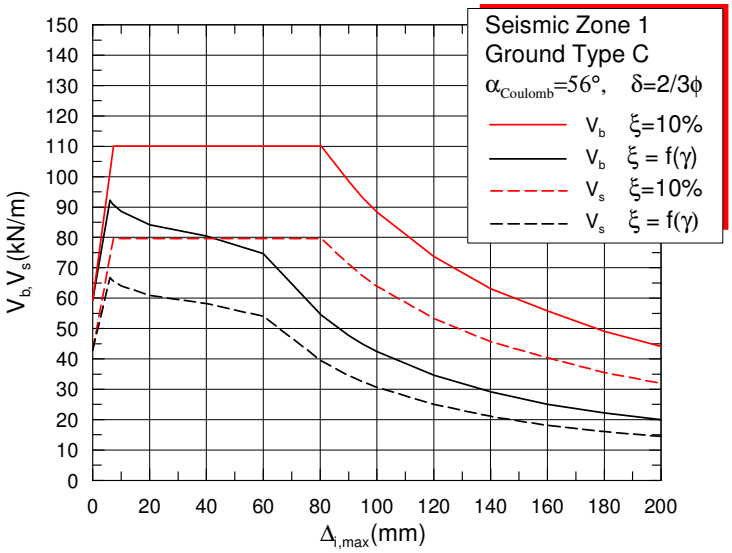

Figure 10b). Dynamic force V_b and V_s *vs*. max. displacement $\Delta_{i,max}$ for ξ = const. and $\xi = f(\gamma)$

4. CONCLUDING REMARKS AND PROSPECTIVE DEVELOPMENTS

From the collection of numerical results discussed in the paper – which are still preliminary – it could be argued that the DBD calculation procedure seems to be very promising in its applicability to retaining structures, such as rigid retaining walls and cantilever diaphragm walls, although these structural typologies were discretized in a very simple manner.

It is noted that an adequate choice of the soil masses participating in the seismic event - *i.e.* the active soil wedge geometry (α) - and the damping ratio, ξ, are fundamental in the calibration of the design procedure.

To this aim, the availability of dynamic numerical analyses as well as well-documented case histories is strongly needed. The research will go on along this direction, in order to better "calibrate" the DBD procedure.

AKNOWLEDGEMENTS

The work is based on the preliminary results of the RELUIS Research Project 2005-2008 "*Sviluppo di approcci agli spostamenti per il progetto e la valutazione della vulnerabilità*". The financial support of the *Dipartimento della Protezione Civile* is gratefully acknowledged.

APPENDIX A

In this very brief section, the analytical expression of the 1st mode of vibration of a cantilever beam of heigth H is reported. The displacement Δ_i, at each depth H - z_i from the top, is given by:

$$\Delta_i = C_1 \left\{ \sin(k_1 z_i) - \sinh(k_1 z_i) + \frac{\cos(k_1 H) + \cosh(k_1 H)}{\sin(k_1 H) - \sinh(k_1 H)} \left[\cos(k_1 z_i) - \cosh(k_1 z_i) \right] \right\}$$

where the constant C_1 is calculated by assuming the maximum displacement $\Delta_{i,\max}$ occurring at the top of the wall, *i.e.:*

$$\Delta_i = \Delta_{i,\max} \frac{z_i}{H} .$$

It follows:

$$C_1 = \frac{\Delta_{i,\max}}{\left\{ \sin(k_1 H) - \sinh(k_1 H) + \frac{\cos(k_1 H) + \cosh(k_1 H)}{\sin(k_1 H) - \sinh(k_1 H)} \left[\cos(k_1 H) - \cosh(k_1 H) \right] \right\}}$$

where $k_1 H = 1.875$ for the 1st mode of vibration.

REFERENCES

EN 1998-1. Eurocode 8: "Design of structures for earthquake resistance – Part 1: General rules, seismic actions and rules for buildings". CEN European Committee for Standardization, Bruxelles, Belgium, Dec. 2003

EN 1998-5). Eurocode 8: Eurocode 8: “Design of structures for earthquake resistance – Part 5: Foundations, retaining structures and geotechnical aspects”. CEN European Committee for Standardization, Bruxelles, Belgium, Dec. 2003

Gulkan, P. and Sozen, M. "Inelastic response of reinforced concrete structures to earthquake motions", ACI Journal 71/12), 604-610, 1974.

Mononobe, N., Matsuo, H. "On the determination of earth pressures during earthquakes". Proceedings World Engineering Conference, Tokyo, Japan, Vol. 9, Paper No. 388, 1929.

Okabe, S. (1926). "General theory of earth pressure and seismic stability of retaining wall and dam". Journal Japanese Society Civil Engineering, Tokyo, Japan, 12(1), 1924.

OPCM 3274, Ordinanza del Presidente del Consiglio dei Ministri (20 Marzo 2003) “Primi elementi in materia di criteri generali per la classificazione sismica del terreitorio nazionale e di normative tecniche per le costruzioni in zona sismica. Supplemento ordinario alla “Gazzetta Ufficiale” n.105, 8 Maggio 2003.

Priestley, M.J.N. "Direct displacement-based design fundamental considerations", Course Material from Fundamentals of Seismic Risk (Rose School), Pavia, Italy, 2001.

Priestley, M.J.N. "Myths and fallacies in Earthquake Engineering, Revisited", The Mallet Milne Lecture, IUSS Press, Pavia, Italy, 2003.

Priestley, M.J.N. "Myths and fallacies in earthquake engineering: conflicts between design and reality", Bulletin, NZ National Society for Earthquake Engineering, New Zealand 26(3), 329-341, 1993.

Priestley, M.J.N. and Kowalsky, MJ. "Direct displacement-based seismic design of concrete building", Bulletin, NZ National Society for Earthquake Engineering, New Zealand 33(4), 421-444, 2000.

Shibata, A. and Sozen, M. "Substitute structure method for seismic design in reinforced concrete", Journal Structural Division, ASCE 102(12), 3548-3566, 1976.

Simonelli, A.L. “La progettazione geotecnica con gli Eurocodici: muri a gravità e diaframmi”, XX Ciclo delle Conferenze Geotecniche di Torino, Novembre 2005.

Sullivan, T.J., Priestley, MJN. and Calvi, GM. “Development of an innovative seismic design procedure for frame-wall structures”, Journal of Earthquake Engineering, vol. 9, Special Issue 2, 279-307, 2005.

Vucetic, M. and Dobry, R. “Effects of the soil plasticity on cyclic response”. Journal of Geotechnical Engineering Division, ASCE, Vol. 117, n. 1, 1991.

Zarrabi-Kashani, K. “Sliding of gravity retaining wall during earthquakes considering vertical accelerations and changing inclination of failure surface”, S,M Thesis., Department of Civil Engineering, Massachusetts Institute of Technology, Cambridge, Massachusetts, 1979.